Tubulin tyrosination is a major factor affecting the recruitment of CAP-Gly proteins at microtubule plus ends.

Leticia Peris, Manuel Thery, Julien Fauré, Yasmina Saoudi, Laurence Lafanechère, John Chilton, Phillip Gordon-Weeks, Niels Galjart, Michel Bornens, Linda Wordeman, et al.

Tubulin tyrosination is required for the recruitment of CAP-Gly microtubule plus-end-tracking proteins at microtubule ends

Leticia Peris[1], Annie Andrieux[1], Manuel Thery[2], Julien Fauré[1], Yasmina Saoudi[1], Laurence Lafanechère[1], John K. Chilton[3], Phillip Gordon-Weeks[3], Niels Galjart[4], Michel Bornens[2], Linda Wordeman[5], Juergen Wehland[6], Didier Job[1].

[1]Laboratoire du Cytosquelette, INSERM U366, Département Réponse et Dynamique Cellulaire, CEA-Grenoble, 17 Rue des Martyrs, 38054 Grenoble, France

[2] Biologie du cycle cellulaire et de la motilité, UMR144, CNRS, Institut Curie, 26 rue d'Ulm 75248 Paris Cedex 05, France.

[3]MRC Centre for Developmental Neurobiology, Kings College London, 4th floor New Hunts House, Guy Campus, London Bridge SE1 1UL, United Kingdom.

[4]Department of Cell Biology and Genetics, Erasmus MC, P.O. Box 1738, 3000 DR Rotterdam, The Netherlands

[5]Department of physiology and Biophysics, University of Washington, Seattle, Washington, 98195

[6]Department of Cell Biology, German Research Center for Biotechnology (GBF), Mascheroder Weg 1, D-38124 Braunschweig, Germany

Correspondance email: didier.job@cea.fr

Phone: 33-438-78-2148; fax: 33-438-78-5057

Running title: tubulin tyrosination and microtubule tip complexes

Keys words: microtubules tubulin-tyrosine-ligase, tyrosination, CLIP-170, p150 Glued, EB1.

Total character count: 42036.

Abstract :

Tubulin-tyrosine-ligase (TTL), the enzyme which catalyzes the addition of a C-terminal tyrosine residue to alpha-tubulin in the tubulin tyrosination cycle, is involved in tumor progression and has a vital role in neuronal organization. We show that in mammalian fibroblasts, CLIP-170, and other microtubule tip tracking proteins comprising a CAP-Gly microtubule-binding domain such as CLIP-115 and p150 Glued, localize to the tips of tyrosinated microtubules but not to the tips of detyrosinated microtubules. *In vitro*, the head domains of CLIP-170 and of p150 Glued bind more tightly to tyrosinated microtubules than to detyrosinated polymers. In TTL null fibroblasts, tubulin detyrosination and CLIP-170 mis-localization correlate with defects in both spindle positioning during mitosis and cell morphology during interphase. These results indicate that tubulin tyrosination regulates microtubule interactions with CAP-Gly microtubule tip proteins and provide explanations for the involvement of TTL in tumor progression and in neuronal organization.

Introduction

In most eucaryotic cells, the C-terminus of alpha tubulin is subject to a cycle of detyrosination-tyrosination in which the C-terminal tyrosine residue of alpha tubulin is sequentially cleaved from the peptide chain by a carboxypeptidase (TCP) and re-added to the chain by the tubulin-tyrosine-ligase (TTL) (Barra et al., 1988; Ersfeld et al., 1993). In both animal models and human cancers, TTL is often suppressed during tumor growth, indicating that TTL suppression and resulting tubulin detyrosination represent a strong selective advantage for proliferating transformed cells (Kato et al., 2004; Lafanechere et al., 1998; Mialhe et al., 2001). In whole animals, TTL is essential for neuronal organization: TTL null mice die within hours after birth due to the disorganization of vital neuronal circuits (Erck et al., 2005). In *S.cerevisiae*, where the tyrosination cycle does not occur but where the structure of the alpha tubulin C-terminus is conserved, removal of the C-terminal aromatic residue of alpha tubulin (a phenylalanine in yeast instead of a tyrosine) disables the interaction of microtubule + tips with Bik1p, the yeast equivalent of the mammalian microtubule + tip tracking protein CLIP-170 (Badin-Larcon et al., 2004). Consistent with a role of tubulin tyrosination in CLIP-170 localization, CLIP-170 is mis-localized in TTL null neurons, being absent from the distal part of neurites and from growth cones (Erck et al., 2005).

In this study, we have used TTL null fibroblasts to probe the influence of tubulin tyrosination on the recruitment of CLIP-170 and of other microtubule + tip proteins (+TIPs), at microtubule ends. We find that tubulin tyrosination is required for proper localization of microtubule +TIPs such as CLIP-170, CLIP-115 or p150 Glued, which comprise at least one CAP-Gly microtubule-binding motif (Accession Number: PF01302; Bateman et al., 2004; Li et al., 2002), whereas other microtubule +TIPs such as EB1, EB3, CLASP or MCAK, interact similarly with tyrosinated or detyrosinated polymers. We provide evidence that tubulin

detyrosination affects directly the interaction between microtubules and CAP-Gly +TIPs, and results in abnormalities in spindle positioning and in cell morphology.

Results

Tubulin tyrosination in WT and TTL null fibroblasts

We have previously shown that interphasic TTL null cells contain massive amounts of detyrosinated (Glu) tubulin but also variable amounts of tyrosinated (Tyr) tubulin, originating from tubulin synthesis (Erck et al., 2005). Here, we have examined the patterns of tubulin tyrosination in relation to the cell cycle in WT or TTL null fibroblasts. When double stained for Tyr tubulin and Glu tubulin, interphasic WT cells displayed extensive tyrosination of cytoplasmic microtubules (MTs), with only a small subset of Glu MTs (Figure 1A), known to correspond to poorly dynamic polymers (Gundersen et al., 1984; Kreis, 1987; Wehland and Weber, 1987). Interphase TTL null fibroblasts contained extensive arrays of Glu MTs and variable amounts of Tyr tubulin (Figure 1A). In four independent experiments, 11%-15% of TTL null fibroblasts were Tyr tubulin negative, displaying only background signal when stained with Tyr tubulin antibody (Tyr–, Figure 1A, B), 50%-60% of the cells showed weak Tyr tubulin staining with mostly discontinuous MT staining (Tyr+, Figure1A, B), and 30%-40% of the cells showed distinct staining of the whole MT network (Tyr+ +, Figure 1A, B). All Tyr tubulin negative cells were also negative for the G2/S marker cyclin A (Furuno et al., 1999) indicating that all were G1 cells (Figure 1C). In a series of control experiments (not shown), in which MT stability was probed using cell exposure to the drug nocodazole, the bulk of cytoplasmic MTs in all WT or TTL null cells were nocodazole sensitive, indicating that in interphase TTL null cells, MT detyrosination was not due to increased MT stability.

In WT mitotic cells, Tyr tubulin antibody stained both the central region of the spindle and the cell periphery, which contains a free tubulin pool and astral MTs. The Glu tubulin signal was low, with a distinct staining of centrioles (Figure 1D). In TTL null mitotic cells, the Tyr tubulin signal was evident in prophase and remained strong through the whole mitotic process (Figure 1D). In metaphase or anaphase cells, spindle MTs were stained with both Tyr tubulin

and Glu tubulin antibody. Interestingly, in all metaphase cells examined, Tyr tubulin staining was apparently restricted to the central region of the spindle, with no detectable signal at the periphery of the cell, where Glu tubulin staining yielded both a diffuse signal corresponding to the soluble tubulin pool and a distinct staining of astral MTs. The uneven distribution of the Tyr tubulin signal among core spindle MTs, astral MTs, and the soluble tubulin pool could result from staining artefacts. However, the same Tyr tubulin antibody which did not stain astral MTs in metaphase TTL null cells always showed a distinct staining of metaphase astral MTs in WT cells (Figure 1D).

Taken together, these results indicate that tubulin detyrosination is maximal in G1 TTL null cells, where they can lack detectable tyrosinated tubulin. Tyr tubulin is present in G2/S and throughout mitosis. Additionally, in metaphase TTL null cells, Tyr tubulin seems to be specifically recruited to core spindle MTs, which include the slowly treadmilling kinetochore-to-pole fibers (Mitchison, 1989). Tyr tubulin is apparently depleted in the soluble tubulin pool and in the astral MTs which are in dynamic equilibrium with this free tubulin pool.

CLIP-170 localization in TTL null fibroblasts

Previous evidence suggests that CLIP-170 association with MT ends is inhibited by tubulin detyrosination, whereas EB1 localization is un-affected (Badin-Larcon et al., 2004; Erck et al., 2005). To asses CLIP-170 localization, WT or TTL null cells were transfected with GFP-CLIP-170 cDNA and then double stained with GFP and EB1 antibodies. In interphase WT cells, GFP-CLIP-170 labelling was widespread in the cells with most EB1 positive MT tips being also positive for GFP-CLIP-170 (Figure 2A). In 30%-45% of the interphase TTL null cells (CLIP-170 + + cells), MT tips also showed GFP-CLIP-170 comets. In 20%-35% of the cells (CLIP-170 + cells), patterns were regionalized, with GFP-CLIP-170 localization at MT ends being restricted to one part of the cell (Figure 2A). Finally, in about 25%-50% of the

cells (CLIP-170– cells), which were often round-shaped, GFP-CLIP-170 failed to associate with MT ends and often formed large cytoplasmic aggregates (Figure 2A). For quantitative analysis of GFP-CLIP-170 localization, 30 EB1 labelled MT ends were selected in each individual cell, examined for GFP-CLIP-170 labelling and the ratio of GFP-CLIP-170 positive MT ends/EB1 positive MT ends was determined. All measurements were performed blind to genotype. In about 50% of the TTL null cells, less than 20% of the EB1 labelled MT ends were CLIP-170 positive (ratio of CLIP-170 positive/EB1 positive MT ends below 0.2), which was never observed in WT cells (Figure 2B). In the remaining population of TTL null cells, GFP-CLIP-170/EB1 ratios had a similar distribution as in WT cells.

We tested the possibility that the lack of CLIP-170 association with growing MT + ends in TTL null cells resulted from transfection artefacts. GFP-CLIP-170 aggregates in CLIP negative cells could result from protein over-expression leading to artefactual perturbations of CLIP-170 localization. However, in WT cells expressing high levels of CLIP-170, the presence of large aggregates did not preclude CLIP-170 association with MT ends (Supplementary figure S1). GFP-CLIP-170 association with MT ends could then be affected by variations in MT growth rates or by tubulin tyrosination *per se*. Video-microscopy experiments (Supplementary figure S2-4) did not support a role of MT growth rates which were similar in WT cells and in TTL null cells, whether or not CLIP-170 was correctly localized (Figure 2C). We then examined whether CLIP-170 localization was linked to tubulin tyrosination in TTL null cells. Cells were transfected with GFP-CLIP-170 and double stained with Tyr tubulin and GFP-antibodies. CLIP-170 localization was scored in 3 classes (+ +, +, –) as above. CLIP-170 scoring was performed blind to the cell tyrosination status. The vast majority of Tyr tubulin negative cells did not contain GFP-CLIP-170 at MT + ends (CLIP-170 – cells, Figure 2D). By contrast, none of the Tyr + + cells was CLIP-170 negative

(Figure 2D). Overall, there was a highly significant relationship between MT tyrosination and CLIP-170 localization (Figure 2D, b).

In WT mitotic cells transfected with GFP-CLIP-170 and double stained for GFP/EB1, many GFP-CLIP-170 and EB1 comets were visible (Figure 3). Interestingly, in TTL null mitotic cells, which contain abundant Tyr tubulin, GFP-CLIP-170 comets were also conspicuous during most phases of mitosis, with the striking exception of metaphase, during which such comets were always lacking.

Taken together our results indicate that, in TTL null cells, MT tyrosination is critical for CLIP-170 association with MT ends with the remarkable exception of spindle metaphase MTs which are tyrosinated and yet lack GFP-CLIP-170 comets (Figure 3). These metaphase Tyr MTs may correspond mainly to kinetochore-to-pole fibers. One could then expect to see clustered GFP-CLIP-170 comets at the metaphase plate but, in our conditions, such comets were actually indistinct even in WT cells (Figure 3). The lack of astral MT comets in metaphase TTL null cells correlates with the apparent lack of Tyr tubulin in metaphase astral polymers in these cells. GFP-CLIP-170 comets re-appear in late anaphase (Figure 3) presumably due to the redistribution of Tyr tubulin from the disassembling kinetochore-to-pole fibers among other polymers.

Effect of the inhibition or rescue of tubulin tyrosination on CLIP-170 localization in TTL null fibroblasts

We used experimental manipulation of the tubulin tyrosination level in TTL null cells to test the causal nature of the relationship between tubulin tyrosination and CLIP-170 localization. For Tyr tubulin depletion we made use of previously described alpha tubulin siRNA which suppress alpha tubulin synthesis and thereby Tyr tubulin pool in TTL null cells (Erck et al., 2005). WT controls or TTL null fibroblasts were transfected with GFP-CLIP-170 and exposed

to alpha tubulin siRNA. These siRNAs have no effect on tubulin tyrosination in WT cells where tubulin is tyrosinated by TTL. In these cells, the MT network was somewhat disorganized (Erck et al., 2005 and figure 4A), but MT ends remained uniformly positive for GFP-CLIP-170. In contrast, alpha tubulin siRNAs induced extensive suppression of tyrosinated tubulin in TTL null cells (figure 4 A, B) in which most MT ends were CLIP-170-negative (Figure 4A, C). Conversely, co-transfection of TTL null cells with TTL cDNA together with GFP-CLIP-170 increased dramatically both the level of MT tyrosination, and the proportion of cells with CLIP-170 at MT ends (Figure 4 A-C). These results strongly indicate that CLIP-170 mis-localization is causally related to tubulin detyrosination in TTL null cells.

Differential binding of CLIP-170 head domain to tyrosinated and detyrosinated microtubules

Is the influence of tubulin tyrosination on CLIP-170 interaction with MTs direct or indirect? To approach this question, we examined the interaction of the CLIP-170 head domain, which contains the CAP-Gly motifs of CLIP-170 (Perez et al., 1999; Scheel et al., 1999), with Tyr or Glu MTs. When WT fibroblasts were transfected with a YFP construct (CLIP-HD-YFP) containing the CLIP-170 head domain, both YFP comets and a lengthwise decoration of MTs were observed (Figure 5A). Interestingly, the comets and the lengthwise MT signal were both lacking in TTL null Tyr negative cells (Figure 5A). CLIP-170 head domain (His-CLIP-170H1) was then added to solutions of affinity-purified Tyr or Glu tubulin (Paturle et al., 1989). Subsequently, tubulin polymerization was initiated and taxol was added to stabilize MTs. Taxol-stabilized MTs were then exposed to increasing NaCl concentrations prior to co-sedimentation assay of CLIP-170 with MTs, which is a standard procedure to measure the stringency of interaction of MTs with MT binding proteins (Bulinski et al., 1999). At low

ionic strength, the CLIP-170 head domain bound to both Tyr and Glu MTs. Interestingly, the CLIP-170 head domain began to be eluted from Glu MTs at 100 mM NaCl (Figure 5B, **), and was almost completely dissociated from MTs at 200mM NaCl (Figure 5B, ##), whereas, at similar NaCl concentrations, the bulk of CLIP-170 head domain was still associated with Tyr MTs (Figure 5B).

These results indicate a direct influence of tubulin tyrosination on CLIP-170 interaction with MTs. We note that CLIP-170 fails to bind to Glu MTs at intracellular NaCl concentrations (150 mM).

Tubulin tyrosination affects microtubule interaction with CAP-Gly tip tracking proteins.

The CAP-Gly microtubule-binding domain of CLIP-170 is also present in the MT tip tracking proteins CLIP-115 and p150 Glued. The head domains of CLIP-115 and of CLIP-170 are homologous, and in this study, in all qualitative and quantitative cellular assays, CLIP-115 behaved like CLIP-170, binding to Tyr but not to Glu MTs (Figure 6A and data not shown). Interestingly, p150 Glued also behaved like CLIP-170. In *in vitro* MT binding assays, a differential binding of p150 Glued to Tyr or Glu MTs was always detectable, although less evident than in the case of CLIP-170 (Figure 6B). We have shown above that, in contrast, EB1 and EB3, two highly related proteins whose MT binding domain does not comprise a CAP-Gly motif, are unaffected by MT tyrosination *in vivo* (Figure 2-6, S2-4). MCAK, which has recently been shown to tip track MTs (Moore et al., 2005), and CLASPs, a previously identified +TIP (Akhmanova et al., 2001), also decorated MT + tips in Tyr negative TTL null cells (Figure 6A). We conclude that tubulin tyrosination affects MT interactions with CAP-Gly +TIPs, in the absence of obvious effects on the behaviour of other +TIPs.

Cell morphology in TTL null fibroblasts

CAP-Gly +TIPs are involved in MT interactions with the cell membrane (Akhmanova et al., 2001; Brunner and Nurse, 2000; Busch and Brunner, 2004; Komarova et al., 2002; Lansbergen et al., 2004; Mimori-Kiyosue et al., 2005) and there is evidence that tubulin detyrosination affects cell morphogenesis in neurons (Erck et al., 2005). In this study, we used a standard shape factor (defined by $4\pi A/P^2$ where A means the area and P the perimeter in Metamorph Software) for quantitative analysis of cell shape. This shape factor varies from 0 to 1, for elongated or circular shapes, respectively. Compared to WT cells, CLIP negative TTL null cells had an increased shape factor, indicative of a more regular, round, shape (Figure 7A a-b). CLIP positive TTL null cells had an average shape factor comparable to that of WT cells, although there was an excess population of cells with a low shape factor (Figure 7A a-b), indicative of irregular and elongated cell shape.

It has been suggested that the presence of CLIP-170 at MT tips is important for MT dependent regulations of actin assemblies, such as lamellipodia (Fukata et al., 2002; Gundersen, 2002). Normal fibroblasts display a distinct polarity by extending a single lamellipodium in the direction of cell migration (Pollard and Borisy, 2003). Accordingly, most WT cells revealed such a pattern (Figure 7B a). In contrast, similar cell polarity was lacking in Tyr negative TTL null cells (Figure 7B a). In Tyr positive TTL null fibroblasts, cells often displayed numerous extensions with several large lamellipodia and resulting conspicuously irregular cell shape (Figure 7B a). In a quantitative analysis, the ratio of the perimeter of large lamellipodia extensions to the total cell perimeter was dramatically diminished in Tyr negative TTL null cells compared to other cells (Figure 7B b), and the number of large lamellipodia extensions per cell was increased in Tyr positive TTL null cells, compared to WT cells (Figure 7B c).

We conclude that cell morphology is perturbed in TTL null cells, probably due to abnormalities in cell polarity, which seems inhibited in Tyr negative cells and disorganized in Tyr + + cells.

Defects in spindle positioning in mitotic TTL null fibroblasts

We used printed micro-patterns of fibronectin to study spindle positioning in WT or TTL null fibroblasts. Micro-patterns constrain extra-cellular matrix organization and thereby organization of both actin assemblies and cell adhesions, which are important for spindle positioning (Thery et al., 2005). We observed similar organization of actin assemblies or of cell adhesions in TTL null cells and WT cells placed on micro-patterns (data not shown). Spindle positioning then depends crucially on astral MT interactions with the metaphase cell cortex (Thery et al., 2005). These interactions involve CAP-Gly +TIPs (Busson et al., 1998), which fail to associate with astral MT ends in TTL null cells.

The majority of mitotic spindles of WT cells grown on **L** shaped patterns were oriented along the hypotenuse (Figure 8A, a-c). In contrast, there was a wide dispersion of spindle orientations in TTL null cells (Figure 8A, d-f), with about 70% of the spindle angle deviating by more than 15° from the median angle compared to only 30% in WT cells (Figure 8B), indicating an impaired control of spindle positioning in TTL null cells.

Discussion

In this study, we show that tubulin tyrosination is central for MT interaction with CAP-Gly +TIPs, and that, in cells, TTL suppression and resulting tubulin detyrosination affect spindle positioning and cell morphology.

Tyrosinated tubulin is not fully suppressed in TTL null cells (Erck et al., 2005), where Tyr tubulin arises from synthesis of new tubulin molecules. Tyr tubulin levels vary in interphase cells that can exhibit complete detyrosination. In contrast, mitotic cells always contain tyrosinated tubulin. The constant presence of Tyr tubulin in mitotic TTL null cells compared to interphase TTL null cells is intriguing. We do not know whether this uniform presence of Tyr tubulin reflects an increased tubulin synthesis when cells enter mitosis, or an inhibition of TCP or both.

Our data provide preliminary but convergent evidence for a preferential recruitment of Tyr tubulin in kinetochore-to-pole MTs compared to Glu tubulin, in TTL null cells. Recent work in *Drosophila* indicates that tubulin incorporation in the treadmilling kinetochore-to-pole MTs during metaphase depend on specific regulations which require CLASP (Mathe et al., 2003). Possibly, tubulin incorporation in kinetochore-to-pole fibers also requires CAP-Gly proteins or other unknown proteins whose interaction with MTs depends on tubulin tyrosination, which would account for the selective recruitment of Tyr tubulin in the core spindle, in TTL null cells. We do not know whether mitotic cells could tolerate the complete suppression of tyrosinated tubulin. We have observed fully detyrosinated mitotic cells in siRNA experiments (not shown). In these cells the spindle was conspicuously disorganized but we found it hard to know whether spindle anomalies were due to tubulin detyrosination *per se* or to other dysfunctions related to the inhibition of alpha tubulin synthesis.

In TTL null cells, tubulin detyrosination affects the recruitment of CAP-Gly proteins at MT ends whereas EB1 localization is unaffected. Additionally, we observe that tubulin tyrosination affects the interaction of MTs with CAP-Gly +TIPs in purified systems, *in vitro*. Clearly, as suggested by previous studies (Badin-Larcon et al., 2004; Galjart and Perez, 2003; Perez et al., 1999), CLIP-170 and p150 Glued localization at MT ends depends crucially on direct interactions between these +TIPs and MTs, even if interactions between both proteins and their interaction with EB1 may also be involved (Akhmanova and Hoogenraad, 2005; Hayashi et al., 2005; Lansbergen et al., 2004; Vaughan et al., 1999). Interestingly, a likely structural basis for the remarkable influence of tubulin tyrosination on CAP-Gly +TIPs interaction with tubulin has recently arisen from a study of the interaction of EB1 with p150 Glued (Hayashi et al., 2005). The EB1 C-terminus is identical to alpha tubulin C-terminus and the C-terminal tyrosine of EB1 has a crucial contribution in its interaction with the CAP-Gly domain of p150 Glued (Hayashi et al., 2005). Very recently, a similar role of the C-terminal tyrosine of EB1 has been reported in the case of EB1 interaction with CLIP-170 (Komarova et al., 2005). Thus, the role of the C-terminal aromatic residue of EB1 and of alpha tubulin in regulating interactions with CAP-Gly +TIPs is apparently conserved among organisms, from yeast to mammals, and may concern additional CAP-Gly proteins (Bateman et al., 2004; Li et al., 2002).

TTL suppression in fibroblasts compromises spindle positioning in cells placed on micro-patterned matrix. Recent studies have shown that metaphase spindle positioning in cells grown on micro-patterns depends both on the organization of the ECM, which is controlled by the micro-pattern, and on astral MT interactions with the cell cortex (Thery et al., 2005). Such interactions are mediated by molecular complexes involving CLIP-170 (or CLIP 115) and p150 Glued (Busson et al., 1998; Coquelle et al., 2002). It is likely that the inhibition of CAP-

Gly +TIPs interaction with detyrosinated astral MTs in TTL null cells accounts for the impaired control of spindle positioning.

TTL suppression also affects the control of cell shape and of cellular extensions in fibroblasts. In fully detyrosinated cells, where CAP-Gly proteins do not interact with MT ends, cell polarization is diminished, and this agrees with previous work indicating a central role of CLIP-170 in MT dependent regulations of actin assemblies (Fukata et al., 2002). In TTL null cells containing enough Tyr tubulin to localize CAP-Gly +TIPs properly, the cell morphology was still perturbed, with multiple cell extensions and an irregular shape. May be there are subtle perturbations of CAP-Gly TIP function in such cells where MTs are still extensively detyrosinated, or tubulin detyrosination may affect proteins other than +TIPs. These possibilities are under examination in our laboratories.

What is the relationship of the phenotypes observed in TTL null fibroblasts with the role of TTL in tumor progression and in brain development? Impaired control of spindle positioning has previously been proposed as one factor favoring tumor invasiveness (Vasiliev et al., 2004). In TTL null tissues in mice, putative defects in spindle positioning due to tubulin detyrosination are apparently compensated, may be through the action of geometrical constraints (Yu et al., 2000). The situation may be different in the brain where TTL null mice display variable degree of ventricle enlargement indicative of cell loss (Erck et al., 2003; Erck et al., 2005). Spindle positioning in neuronal progenitors is a complex and highly regulated process crucial for the control of progenitors proliferation/differentiation in the neuronal epithelium (Faulkner et al., 2000; Haydar et al., 2003). Spindle positioning could be perturbed in TTL null mice with resulting abnormalities in neuronal differentiation/proliferation equilibrium. With regard to the control of cell morphology, our data are consistent with studies that indicate an important role of CAP-Gly +TIPs for the control of cell shape (Brunner and Nurse, 2000{Fukata, 2002 #795; Fukata et al., 2002; Gundersen, 2002). Such

defects in cell shape control are apparently compensated in TTL null non-neuronal tissues, which are apparently normal, whereas they are probably deleterious in neurons, which exhibit an erratic time course of neurite extensions (Erck et al., 2005). Neuronal cells may be especially sensitive to defects in cell shape controls, given the extreme size and complexity of neurite extensions. Finally, our data suggest that defects in cell shape may be associated with alterations of cell polarity. Such defects may affect cell motility as well as cell-ell or cell-matrix adhesions, which could be involved in the facilitating effect of tubulin de-tyrosination on tumor growth.

Our data demonstrate that tubulin tyrosination is essential for MT interaction with CAP-Gly proteins, but do not give definite clues to understand why a great number of eucaryotic cells developed a tyrosination cycle by introducing a detyrosination reaction. The bulk of tubulin is detyrosinated in differentiated cells (Gundersen et al., 1984), and it may be the case that tubulin detyrosination is used to disconnect MT-membrane interactions, in terminally differentiated cells which do not need to change shape or divide any longer. The identification of TCP and subsequent TCP suppression will be necessary for a full understanding of the tyrosination cycle. Clearly though, this cycle is an important aspect of MT physiology, being involved in MT functions which are conserved, vital, and important for tumor progression.

Materials and methods

Antibodies

Primary antibodies: Glu tubulin (Paturle-Lafanechere et al., 1994), Tyr tubulin (clone YL1/2, (Wehland and Weber, 1987); EB1 (BD Transduction Laboratories), GFP (Molecular Probes), Cyclin A (Clone CY-A1, SIGMA).

Cell culture and immunofluorescence microscopy

Mouse embryonic fibroblasts (MEFs) were prepared from E13.5 embryos, as previously described (Erck et al., 2005). Cells were maintained at 37°C with 5%CO2 and 3% O2.

Immunofluorescence procedure: after fixation (-20C methanol or 4 % PFA containing 4.1% sucrose, followed by cell permeabilization with 0.1 % Triton X–100 in PBS) and incubation with primary antibodies, cells were incubated with either Cy3, Cy5 (Jackson Immunoresearch laboratories) or Alexa 488 (Molecular Probes) secondary antibodies. To visualize F-actin, rhodamine-phalloidin (Molecular Probes, Eugene, OR) was included with the secondary antibody.

Fluorescence images were captured with a CoolSnap ES charge-coupled device camera (Roper Scientific, Trenton, NJ) in a straight microscope (Axioskop 50, Zeiss) controlled by Metaview software (Universal Imaging Corp). When necessary, images were scanned using a piezo device adapted to a 100x/1.3 PL-Neofluor objective and treated by deconvolution microscopy using calculated point spread function.

Cell transfection

GFP-CLIP-170 cDNA was provided by Dr F.Perez, (Curie Institute, Paris); EB3-mRFP was provided by Dr V. Small (Vienna, Austria); GFP-CLIP-115 (Hoogenraad et al., 2000); EGFP-p150Glued (Hoogenraad et al., 2001) and GFP-CLASP1 (Akhmanova et al., 2001), GFP-MCAK (Wordeman et al., 1999) has been described. Mouse TTL coding sequence was inserted in pcDNA3 (Invitrogen). CLIP-170 head-YFP, aa 1–278 was generated in pclink vector.

MEF cultures were transfected using 1µg of DNA and Lipofectamine Plus (Invitrogen) following manufacturer's protocol. For co-transfection experiments using RFP and GFP constructs, we used 1µg of total DNA and pilot transfection were performed to determine the

respective proportion of each DNA which lead to transfected cells positives for both RFP and GFP. For rescue experiments, we performed co-transfection with GFP-CLIP-170 and TTL cDNA (ratio 1/4); the efficiency of the co-transfection was evaluated by the presence of both GFP-CLIP-170 protein and of Tyr tubulin (as a result of the presence of TTL).
Anti tubulin siRNA, were used as previously described (Erck et al., 2005).

Micro-pattern fabrication.

L shaped fibronectin micropatterns of 35 μm long were made as described previously (Thery et al., 2005). MEFs were resuspended in DMEM10%SVF and deposited on the printed coverslip at a density of 10^4 cells per cm2.

Time lapse video microscopy

To analyse MT dynamics, we cultured MEFs in 35 mm glass Petri dishes (Iwaki, Dutscher). 48 hrs after co-transfection with GFP-CLIP-170 and EB3-mRFP, cells were placed in a humidified incubator at 37°C with 5% CO2 inside the video microscopy platform. Fluorescent images were captured every 3 seconds with a CoolSnap HQ charge-coupled device camera (Roper Scientific, Trenton, NJ) in an inverted motorized microscope (Axiovert 200M, Zeiss) controlled by MetaMorph software (Universal Imaging, Downingtown, PA). To measure MT growth rate, we quantified EB3-mRFP velocity in more than 30 cells belonging to three independent MEFs culture arising from independent embryos. To analyse mitotic spindle position, MEFs were plated on L shaped fibronectin micropatterns and placed inside the video microscopy platform at 37°C with 5% CO2. Time lapse of Z series images (Z=4) were collected in multi-position in Trans illumination each 3 minutes for 20h. To quantify mitotic angle, we designed a line perpendicular to metaphase plate and we measured the angle between this line and the micropattern hypotenuse using MetaMorph software. More than 60 mitotic angles were analyzed for each experiment.

Preparation of tyrosinated and detyrosinated tubulin

Affinity-purified tyrosinated or detyrosinated tubulin was prepared as previously described (Paturle et al., 1989). For storage, both forms of tubulin were concentrated to at least 5 mg/ml, using centricon 30 and transferred to PEM buffer (pH 6.65, 100 mM PIPES, 1mM EGTA and 1mM $MgCl_2$) made with D_2O instead of H_2O, containing 1mM GTP and 10mM $MgCl_2$. The mixture was stored at -80°C before use. These buffer and storage conditions allow the full

preservation of the polymerization capacities of affinity purified tubulin species (Giraudel et al., 1998).

Protein Purification, Microtubule Polymerization and Co-sedimentation assay

His-CLIP-170 H1 (aa 1-350) cloned into pET19b vector was provided by Dr F.Perez. His-p150Glued head domain (aa 99-296) cloned into pET28 vector has been described (Lansbergen et al., 2004). Both constructs were expressed in bacteria and proteins were purified as described previously (Scheel et al., 1999). Western blot analysis revealed a double band with a molecular weight of 40 kd for His-CLIP-170 H1, and a single band with a molecular weight of 25 kd for His-p150Glued head domain (data not shown).

Prior to co-sedimentation assays, tyrosinated and detyrosinated tubulin were centrifuged for 10 min at 70,000 rpm and 4 °C in a TLA100 Beckman rotor. Microtubule polymerization was performed by incubating Tyr or Glu tubulin with His-CLIP-170 H1 or His-p150Glued (molar ratio of 1/8 and 1/5 respectively) in PEM with 1mM GTP, 5mM $MgCl_2$, and 20% Glycerol at 37°C for 20 min. MTs were stabilized with Taxol and exposed to increasing concentration of salt (0, 100mM and 200mM of NaCl in PEM 20% Glycerol) for 10 min at 37°C. The reaction mixture was ultra-centrifuged in a PEM 60% Glycerol cushion for 30 min at 70000 rpm at 30°C, then, supernatants and pellets were analyzed by SDS PAGE gels and stained with Coomassie blue.

Acknowledgements

This work was supported in part by a grant from Ligue Francaise contre le Cancer (equipe labellisee Ligue) to DJ, by grants from the Netherlands Ministry of Economic Affairs (BSIK) and the Dutch Cancer Society (KWF) to NG; by NIH grant GM69429 to LW and the Deutsche Forschungsgemeinschaft to JW. We thank D. Proietto, A. Schweitzer and C. Bosc for precious help during this work; Dr F. Perez and Dr V Small for advice and for providing CLIP170 and EB3 constructions respectively. L. Peris is supported by a post-doctoral fellowship from the “Fondation pour la Recherche Medicale”.

Abbreviations list

MT: Microtubule; **+TIPs:** Microtubule + tip tracking proteins**; TTL:** Tubulin-tyrosine-ligase**; Tyr tubulin:** Tyrosinated tubulin**, Glu tubulin:** Detyrosinated tubulin**, CAP-Gly:** Cytoskeleton-associated protein glycine-rich domain**; TCP:** Tubulin carboxypeptidase**, MCAK:** Mitotic centromere-associated kinesin**, CLIPs:** Cytoplasmic linker proteins; **CLASP:** CLIP-associating protein**; WT**: Wild type**; TTL KO:** Tubulin-tyrosine-ligase null.

References

Akhmanova, A., and C.C. Hoogenraad. 2005. Microtubule plus-end-tracking proteins: mechanisms and functions. *Curr Opin Cell Biol*. 17:47-54.

Akhmanova, A., C.C. Hoogenraad, K. Drabek, T. Stepanova, B. Dortland, T. Verkerk, W. Vermeulen, B.M. Burgering, C.I. De Zeeuw, F. Grosveld, and N. Galjart. 2001. Clasps are CLIP-115 and -170 associating proteins involved in the regional regulation of microtubule dynamics in motile fibroblasts. *Cell*. 104:923-35.

Badin-Larcon, A.C., C. Boscheron, J.M. Soleilhac, M. Piel, C. Mann, E. Denarier, A. Fourest-Lieuvin, L. Lafanechere, M. Bornens, and D. Job. 2004. Suppression of nuclear oscillations in Saccharomyces cerevisiae expressing Glu tubulin. *Proc Natl Acad Sci U S A*. 101:5577-82.

Barra, H.S., C.A. Arce, and C.E. Argarana. 1988. Posttranslational tyrosination/detyrosination of tubulin. *Mol Neurobiol*. 2:133-53.

Bateman, A., L. Coin, R. Durbin, R.D. Finn, V. Hollich, S. Griffiths-Jones, A. Khanna, M. Marshall, S. Moxon, E.L. Sonnhammer, D.J. Studholme, C. Yeats, and S.R. Eddy. 2004. The Pfam protein families database. *Nucleic Acids Res*. 32:D138-41.

Brunner, D., and P. Nurse. 2000. CLIP170-like tip1p spatially organizes microtubular dynamics in fission yeast. *Cell*. 102:695-704.

Bulinski, J.C., D. Gruber, K. Faire, P. Prasad, and W. Chang. 1999. GFP chimeras of E-MAP-115 (ensconsin) domains mimic behavior of the endogenous protein in vitro and in vivo. *Cell Struct Funct*. 24:313-20.

Busch, K.E., and D. Brunner. 2004. The microtubule plus end-tracking proteins mal3p and tip1p cooperate for cell-end targeting of interphase microtubules. *Curr Biol*. 14:548-59.

Busson, S., D. Dujardin, A. Moreau, J. Dompierre, and J.R. De Mey. 1998. Dynein and dynactin are localized to astral microtubules and at cortical sites in mitotic epithelial cells. *Curr Biol*. 8:541-4.

Coquelle, F.M., M. Caspi, F.P. Cordelieres, J.P. Dompierre, D.L. Dujardin, C. Koifman, P. Martin, C.C. Hoogenraad, A. Akhmanova, N. Galjart, J.R. De Mey, and O. Reiner. 2002. LIS1, CLIP-170's key to the dynein/dynactin pathway. *Mol Cell Biol*. 22:3089-102.

Erck, C., R.A. MacLeod, and J. Wehland. 2003. Cloning and genomic organization of the TTL gene on mouse chromosome 2 and human chromosome 2q13. *Cytogenet Genome Res*. 101:47-53.

Erck, C., L. Peris, A. Andrieux, C. Meissirel, A.D. Gruber, M. Vernet, A. Schweitzer, Y. Saoudi, H. Pointu, C. Bosc, P.A. Salin, D. Job, and J. Wehland. 2005. A vital role of tubulin-tyrosine-ligase for neuronal organization. *Proc Natl Acad Sci U S A*.

Ersfeld, K., J. Wehland, U. Plessmann, H. Dodemont, V. Gerke, and K. Weber. 1993. Characterization of the tubulin-tyrosine ligase. *J Cell Biol*. 120:725-32.

Faulkner, N.E., D.L. Dujardin, C.Y. Tai, K.T. Vaughan, C.B. O'Connell, Y. Wang, and R.B. Vallee. 2000. A role for the lissencephaly gene LIS1 in mitosis and cytoplasmic dynein function. *Nat Cell Biol*. 2:784-91.

Fukata, M., T. Watanabe, J. Noritake, M. Nakagawa, M. Yamaga, S. Kuroda, Y. Matsuura, A. Iwamatsu, F. Perez, and K. Kaibuchi. 2002. Rac1 and Cdc42 capture microtubules through IQGAP1 and CLIP-170. *Cell*. 109:873-85.

Furuno, N., N. den Elzen, and J. Pines. 1999. Human cyclin A is required for mitosis until mid prophase. *J Cell Biol*. 147:295-306.

Galjart, N., and F. Perez. 2003. A plus-end raft to control microtubule dynamics and function. *Curr Opin Cell Biol*. 15:48-53.

Giraudel, A., L. Lafanechere, M. Ronjat, J. Wehland, J.R. Garel, L. Wilson, and D. Job. 1998. Separation of tubulin subunits under nondenaturing conditions. *Biochemistry*. 37:8724-34.

Gundersen, G.G. 2002. Microtubule capture: IQGAP and CLIP-170 expand the repertoire. *Curr Biol*. 12:R645-7.

Gundersen, G.G., M.H. Kalnoski, and J.C. Bulinski. 1984. Distinct populations of microtubules: tyrosinated and nontyrosinated alpha tubulin are distributed differently in vivo. *Cell*. 38:779-89.

Hayashi, I., A. Wilde, T.K. Mal, and M. Ikura. 2005. Structural basis for the activation of microtubule assembly by the EB1 and p150Glued complex. *Mol Cell*. 19:449-60.

Haydar, T.F., E. Ang, Jr., and P. Rakic. 2003. Mitotic spindle rotation and mode of cell division in the developing telencephalon. *Proc Natl Acad Sci U S A*. 100:2890-5.

Hoogenraad, C.C., A. Akhmanova, F. Grosveld, C.I. De Zeeuw, and N. Galjart. 2000. Functional analysis of CLIP-115 and its binding to microtubules. *J Cell Sci*. 113 (Pt 12):2285-97.

Hoogenraad, C.C., A. Akhmanova, S.A. Howell, B.R. Dortland, C.I. De Zeeuw, R. Willemsen, P. Visser, F. Grosveld, and N. Galjart. 2001. Mammalian Golgi-associated Bicaudal-D2 functions in the dynein-dynactin pathway by interacting with these complexes. *Embo J*. 20:4041-54.

Kato, C., K. Miyazaki, A. Nakagawa, M. Ohira, Y. Nakamura, T. Ozaki, T. Imai, and A. Nakagawara. 2004. Low expression of human tubulin tyrosine ligase and suppressed tubulin tyrosination/detyrosination cycle are associated with impaired neuronal differentiation in neuroblastomas with poor prognosis. *Int J Cancer*. 112:365-75.

Komarova, Y., G. Lansbergen, N. Galjart, F. Grosveld, G.G. Borisy, and A. Akhmanova. 2005. EB1 and EB3 Control CLIP Dissociation from the Ends of Growing Microtubules. *Mol Biol Cell*. 16:5334-45.

Komarova, Y.A., A.S. Akhmanova, S. Kojima, N. Galjart, and G.G. Borisy. 2002. Cytoplasmic linker proteins promote microtubule rescue in vivo. *J Cell Biol*. 159:589-99.

Kreis, T.E. 1987. Microtubules containing detyrosinated tubulin are less dynamic. *Embo J*. 6:2597-606.

Lafanechere, L., C. Courtay-Cahen, T. Kawakami, M. Jacrot, M. Rudiger, J. Wehland, D. Job, and R.L. Margolis. 1998. Suppression of tubulin tyrosine ligase during tumor growth. *J Cell Sci*. 111 (Pt 2):171-81.

Lansbergen, G., Y. Komarova, M. Modesti, C. Wyman, C.C. Hoogenraad, H.V. Goodson, R.P. Lemaitre, D.N. Drechsel, E. van Munster, T.W. Gadella, Jr., F. Grosveld, N. Galjart, G.G. Borisy, and A. Akhmanova. 2004. Conformational changes in CLIP-170 regulate its binding to microtubules and dynactin localization. *J Cell Biol*. 166:1003-14.

Li, S., J. Finley, Z.J. Liu, S.H. Qiu, H. Chen, C.H. Luan, M. Carson, J. Tsao, D. Johnson, G. Lin, J. Zhao, W. Thomas, L.A. Nagy, B. Sha, L.J. DeLucas, B.C. Wang, and M. Luo. 2002. Crystal structure of the cytoskeleton-associated protein glycine-rich (CAP-Gly) domain. *J Biol Chem*. 277:48596-601.

Mathe, E., Y.H. Inoue, W. Palframan, G. Brown, and D.M. Glover. 2003. Orbit/Mast, the CLASP orthologue of Drosophila, is required for asymmetric stem cell and cystocyte divisions and development of the polarised microtubule network that interconnects oocyte and nurse cells during oogenesis. *Development*. 130:901-15.

Mialhe, A., L. Lafanechere, I. Treilleux, N. Peloux, C. Dumontet, A. Bremond, M.H. Panh, R. Payan, J. Wehland, R.L. Margolis, and D. Job. 2001. Tubulin detyrosination is a frequent occurrence in breast cancers of poor prognosis. *Cancer Res*. 61:5024-7.

Mimori-Kiyosue, Y., I. Grigoriev, G. Lansbergen, H. Sasaki, C. Matsui, F. Severin, N. Galjart, F. Grosveld, I. Vorobjev, S. Tsukita, and A. Akhmanova. 2005. CLASP1 and CLASP2 bind to EB1 and regulate microtubule plus-end dynamics at the cell cortex. *J Cell Biol*. 168:141-53.

Mitchison, T.J. 1989. Polewards microtubule flux in the mitotic spindle: evidence from photoactivation of fluorescence. *J Cell Biol*. 109:637-52.

Moore, A.T., K.E. Rankin, G. von Dassow, L. Peris, M. Wagenbach, Y. Ovechkina, A. Andrieux, D. Job, and L. Wordeman. 2005. MCAK associates with the tips of polymerizing microtubules. *J Cell Biol*. 169:391-7.

Paturle-Lafanechere, L., M. Manier, N. Trigault, F. Pirollet, H. Mazarguil, and D. Job. 1994. Accumulation of delta 2-tubulin, a major tubulin variant that cannot be tyrosinated, in neuronal tissues and in stable microtubule assemblies. *J Cell Sci*. 107 (Pt 6):1529-43.

Paturle, L., J. Wehland, R.L. Margolis, and D. Job. 1989. Complete separation of tyrosinated, detyrosinated, and nontyrosinatable brain tubulin subpopulations using affinity chromatography. *Biochemistry*. 28:2698-704.

Perez, F., G.S. Diamantopoulos, R. Stalder, and T.E. Kreis. 1999. CLIP-170 highlights growing microtubule ends in vivo. *Cell*. 96:517-27.

Pollard, T.D., and G.G. Borisy. 2003. Cellular motility driven by assembly and disassembly of actin filaments. *Cell*. 112:453-65.

Scheel, J., P. Pierre, J.E. Rickard, G.S. Diamantopoulos, C. Valetti, F.G. van der Goot, M. Haner, U. Aebi, and T.E. Kreis. 1999. Purification and analysis of authentic CLIP-170 and recombinant fragments. *J Biol Chem*. 274:25883-91.

Thery, M., V. Racine, A. Pepin, M. Piel, Y. Chen, J.B. Sibarita, and M. Bornens. 2005. The extracellular matrix guides the orientation of the cell division axis. *Nat Cell Biol*. 7:947-53.

Vasiliev, J.M., T. Omelchenko, I.M. Gelfand, H.H. Feder, and E.M. Bonder. 2004. Rho overexpression leads to mitosis-associated detachment of cells from epithelial sheets: a link to the mechanism of cancer dissemination. *Proc Natl Acad Sci U S A*. 101:12526-30.

Vaughan, K.T., S.H. Tynan, N.E. Faulkner, C.J. Echeverri, and R.B. Vallee. 1999. Colocalization of cytoplasmic dynein with dynactin and CLIP-170 at microtubule distal ends. *J Cell Sci*. 112 (Pt 10):1437-47.

Wehland, J., and K. Weber. 1987. Turnover of the carboxy-terminal tyrosine of alpha-tubulin and means of reaching elevated levels of detyrosination in living cells. *J Cell Sci*. 88 (Pt 2):185-203.

Wordeman, L., M. Wagenbach, and T. Maney. 1999. Mutations in the ATP-binding domain affect the subcellular distribution of mitotic centromere-associated kinesin (MCAK). *Cell Biol Int*. 23:275-86.

Yu, F., X. Morin, Y. Cai, X. Yang, and W. Chia. 2000. Analysis of partner of inscuteable, a novel player of Drosophila asymmetric divisions, reveals two distinct steps in inscuteable apical localization. *Cell*. 100:399-409.

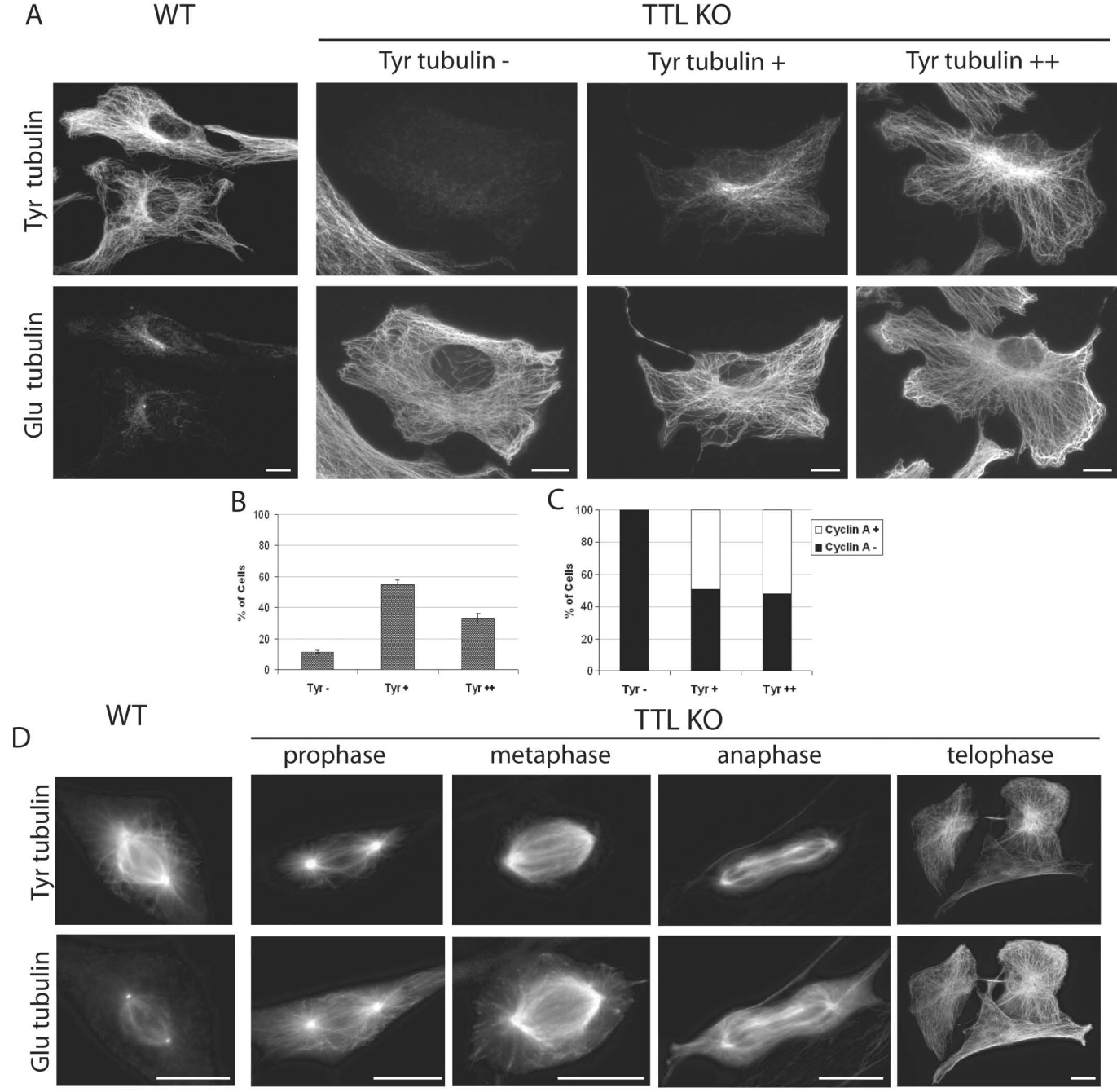

Figure 1: Tubulin tyrosination in WT or TTL KO fibroblasts

(A) Double-immunostaining of Tyr and Glu tubulin in WT or TTL KO interphase fibroblasts. MT network of WT fibroblasts was mainly composed of Tyr tubulin. TTL KO fibroblasts contained extensive arrays of Glu microtubules and variable amounts of Tyr tubulin, scored in three classes: Tyr - : background signal; Tyr+: weak and discontinuous Tyr tubulin staining of microtubules; Tyr+ +: distinct continuous staining of most of the microtubule network. (B) TTL KO fibroblast distribution in the three Tyr tubulin classes (n=308). (C) Proportion of Cyclin A positive cells (S/G2 cells) in Tyr - , Tyr + or Tyr + + interphase TTL KO fibroblasts (n=125). Note that all the Tyr - cells were also Cyclin A negative. (D) Double-immunostaining of Tyr and Glu tubulin in WT and TTL KO mitotic fibroblasts. Note that in metaphase TTL KO mitotic fibroblasts Tyr tubulin is only detectable in central spindle microtubules, whereas astral MTs are composed of Glu tubulin. More than 50 mitotic cells were examined in each genotype. Scale bar 10 um.

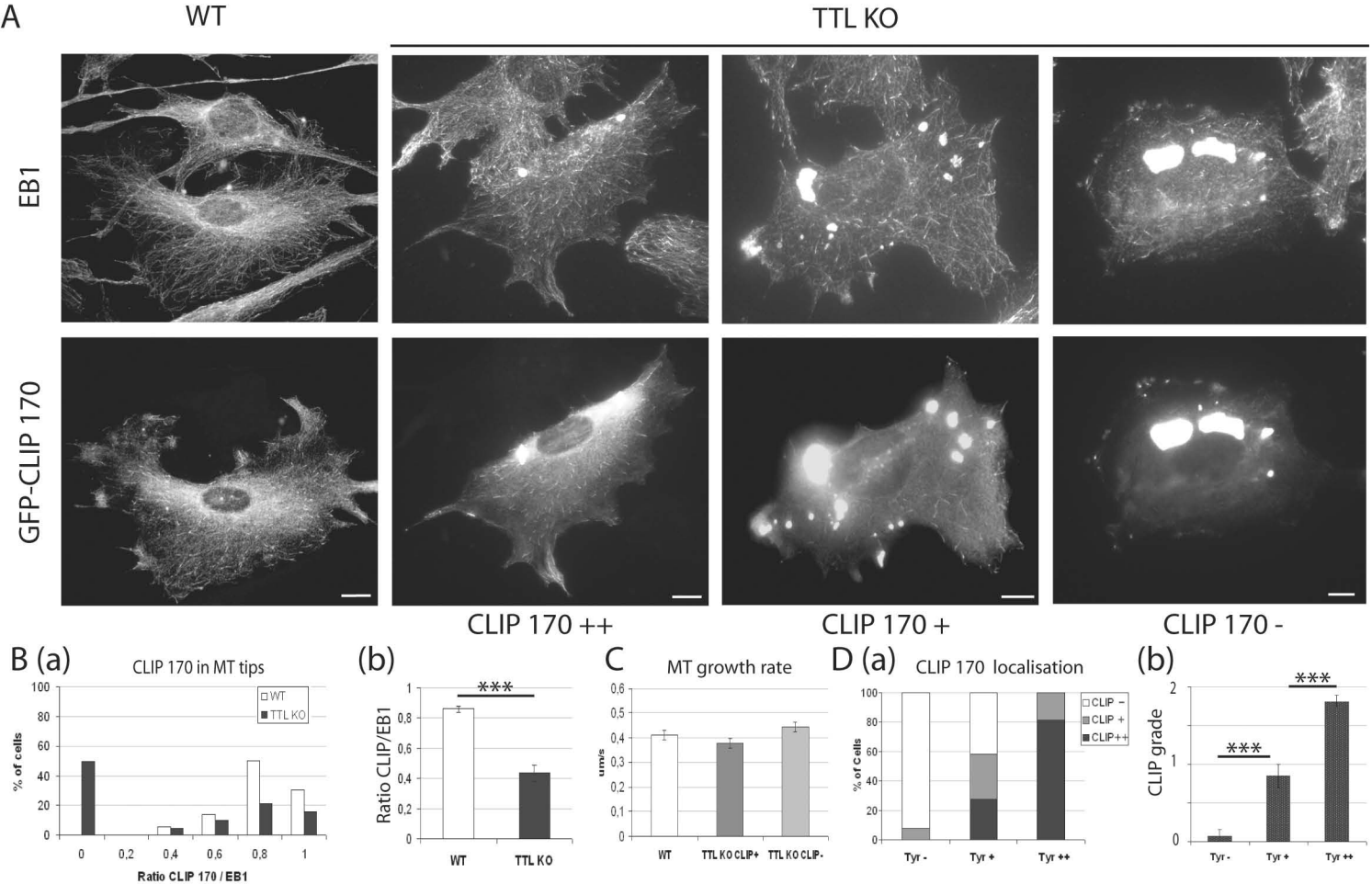

Figure 2: CLIP-170 localization in WT or TTL KO fibroblasts

(A) EB1 and CLIP-170 localization in WT or TTL KO fibroblasts. Fibroblasts were transfected with GFP-CLIP-170 cDNA and double stained with EB1 and GFP antibodies. In WT cells (n=52), CLIP-170 and EB1 co-localized at MT tips. TTL KO fibroblasts (n=98) showed several pattern of CLIP-170 distribution which were scored in three classes: CLIP-170 + +: CLIP-170 at MT tips; CLIP-170 +: MT tip localization of CLIP-170 restricted to a part of the cell; CLIP-170–: no detectable CLIP-170 at microtubule ends (B) Quantitative analysis of CLIP-170 localization in WT or TTL KO fibroblasts. MTs plus ends were identified by EB1 positive signal and the percent of CLIP-170 positive tips within EB1 MTs tips was quantified (ratio CLIP-170/EB1). (a) Distribution of CLIP-170 positive tips in WT (n=36) or TTL KO (n=71) cells. Note that in almost 50% of TTL KO cells CLIP-170 barely associates with MTs tips (ratio CLIP-170/EB1 < 0.2). (b) Mean values + - S.E.M. of the ratio CLIP-170/EB1 in WT or TTL KO cells.*** p<0.001 (t test). (C) MT growth rate measurement in WT or TTL KO cells (mean + - S.E.M.). Cells were double-transfected with GFP-CLIP-170 and EB3 RFP cDNAs and the velocity of microtubule growth was measured using video-microscopy (nWT tips=70; n TTL KO CLIP+ tips=70; n TTL KO CLIP– tips=84; supplementary data S2-S4). (D) Analysis of CLIP-170 MT tip localisation in function of the tyrosination level in TTL KO fibroblasts. (a): proportions of CLIP–, CLIP+ and CLIP+ + cells as a function of the tyrosination level in TTL KO fibroblasts (n=98). (b) Mean value + - S.E.M. of CLIP grade in TTL KO fibroblasts as a function of tubulin tyrosination. CLIP grade was of 0, 1, 2 for CLIP–, CLIP+ and CLIP+ + cells, respectively. *** p<0,001 (t test). Note that the average CLIP-170 grade of Tyr– cells is close to 0 (no CLIP-170 at MTs tips).

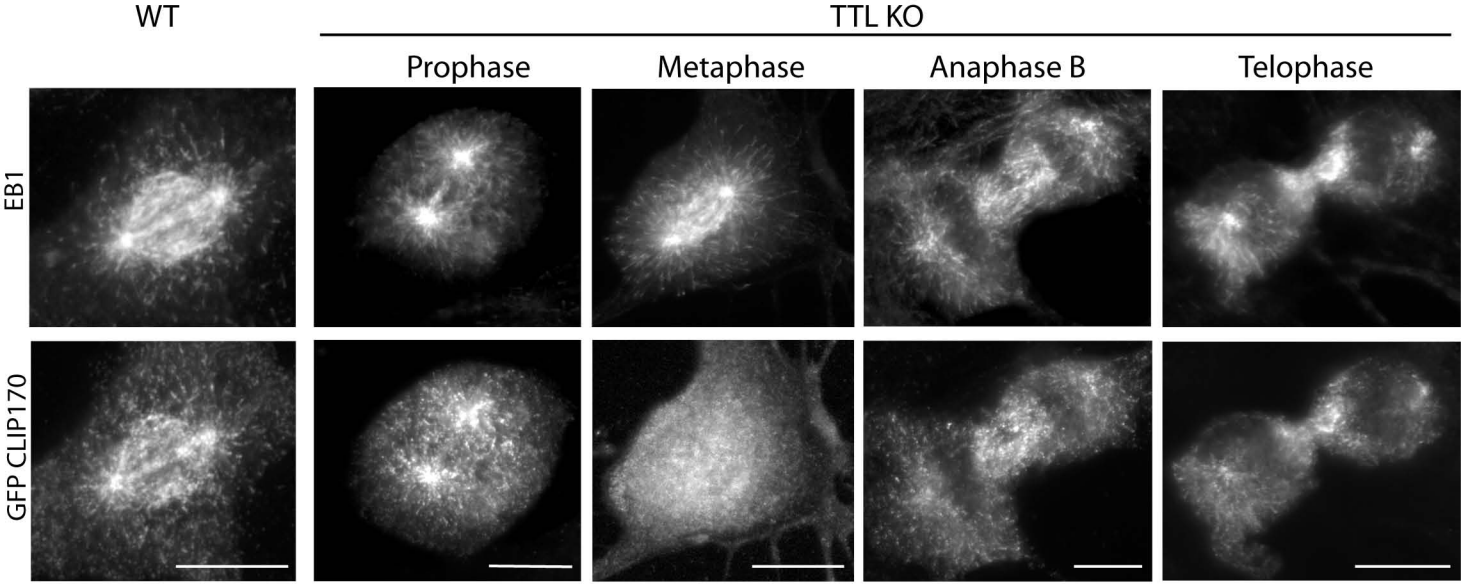

Figure 3: CLIP-170 and EB1 distribution in mitotic spindle

WT or TTL KO fibroblasts were transfected with GFP-CLIP-170 cDNA and double stained with GFP and EB1 antibodies. At least 30 mitotic cells were examined in each genotype. In WT mitotic cells, numerous GFP-CLIP-170 and EB1 comets were evident. GFP-CLIP-170 and EB1 comets were also conspicuous in prophase, late anaphase and telophase TTL KO cells. In contrast, no distinct GFP-CLIP-170 comets were observed in metaphase TTL KO cells. Scale bar 10um.

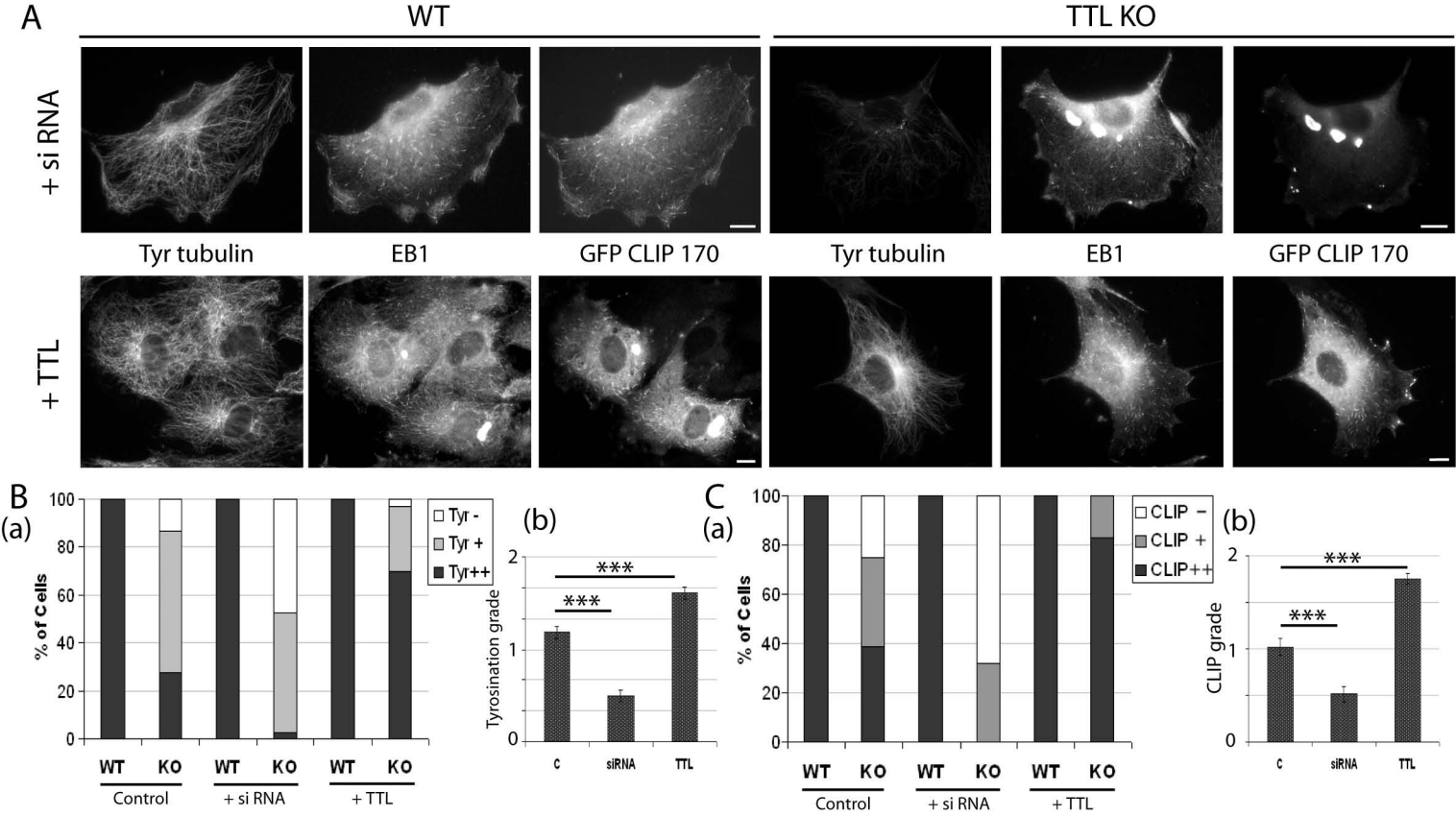

Figure 4: Inhibition or rescue of tubulin tyrosination in TTL null fibroblasts

(A) WT or TTL KO fibroblasts were transfected with GFP-CLIP-170 cDNA and either treated with siRNA against alpha-tubulin (+siRNA) or transfected with TTL cDNA (+TTL). In control experiments, cell transfection with scramble siRNA or TTL vector alone gave similar results, shown as "control". Cells were triple-stained with Tyr tubulin, GFP and EB1 antibodies. Scale bar: 10um. (B) (a) Analysis of tyrosination levels in WT or TTL KO cells (Tyr - , Tyr +, Tyr + +) in non-treated cells (Control WT n=52, Control TTL KO n=98), in cells treated with RNAi against Tyr tubulin (+siRNA WT n=50 ,+siRNA TTL KO n=82) and in cells transfected with TTL (+TTL WT n=50, +TTL TTL KO n=96). In WT cells, treatments had not effect on tubulin tyrosination. In TTL KO cells, Tyr Tubulin siRNA treatment increased the percentage of Tyr – cells as compared to control conditions. (b) Comparison of tubulin tyrosination grades (mean + - S.E.M.). The tyrosination grade was 0, 1,or 2 for Tyr –, Tyr + and Tyr + + cells, respectively, *** $p<0.001$ (t test). TTL cDNA transfection significantly increased the percentage of Tyr + + cells as compared to control conditions. (C) (a) Analysis of CLIP-170 distribution in WT or TTL KO cells, in non-treated cells (Control WT n=52, Control TTL KO n=98), in cells treated with siRNAi against alpha-tubulin (+siRNA WT n=50 ,+siRNA TTL KO n=82) and in cells transfected with TTL cDNA (+TTL WT n=50, +TTL TTL KO n=96). In TTL KO cells, no CLIP+ + cell was observed following exposure to siRNA and no CLIP– cell was observed following TTL cDNA transfection. (b) CLIP-170 grades in TTL KO fibroblasts (mean + - S.E.M.). CLIP-170 grading was as in figure 2. *** $p<0.001$ (t test).

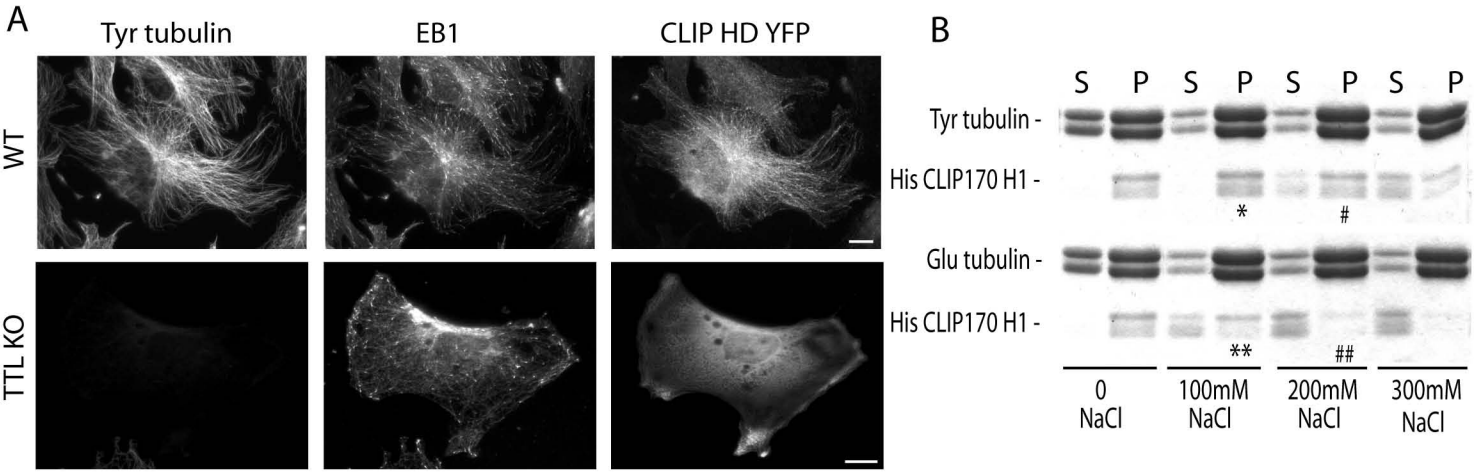

Figure 5: Differential binding of CLIP-170 head domain to Tyr and Glu MTs in vivo and in vitro

(A) Triple staining of Tyr tubulin, EB1 and CLIP-170 head domain in WT or TTL KO fibroblasts transfected with CLIP-170HD-YFP cDNA. In WT cells, over expressed CLIP-170HD-YFP decorated the whole MT network and accumulated at MTs tips. In TTL KO cells Tyr –, CLIP-170HD-YFP remained soluble in the cytoplasm. Scale bar: 10um

(B) Microtubule-binding assay. CLIP-170 head domain (His-CLIP-170 H1) was co-polymerized with Tyr or Glu tubulin. Tyr and Glu-MTs were stabilized with Taxol and incubated with increasing concentrations of NaCl, as indicated. Equal amount of supernatants (S) and pellets (P) were separated by SDS/PAGE and stained with Coomassie blue. His-CLIP-170 H1 shows a double band with a molecular mass of 40 kD. In the presence of 100 mM NaCl, the bulk of His-CLIP-170 H1 remained bound to Tyr-MTs (*) whereas only about half of His-CLIP-170 H1 remained bound to Glu-MTs (**). In the presence of 200 mM NaCl, the majority of His-CLIP-170 H1 was still bound to Tyr-MTs (#) whereas only a small proportion of His-CLIP-170 H1 remained bound to Glu-MTs (##).

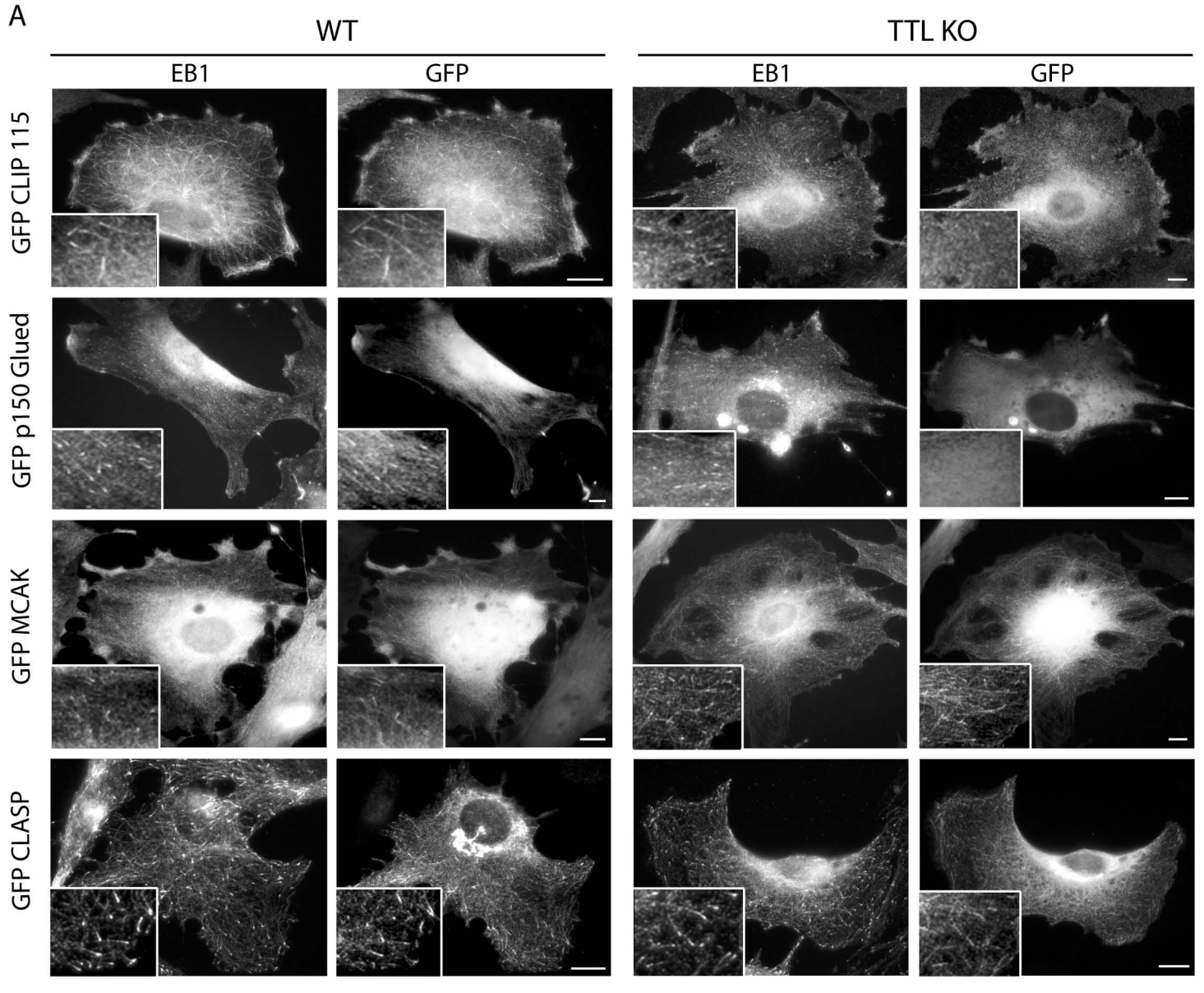

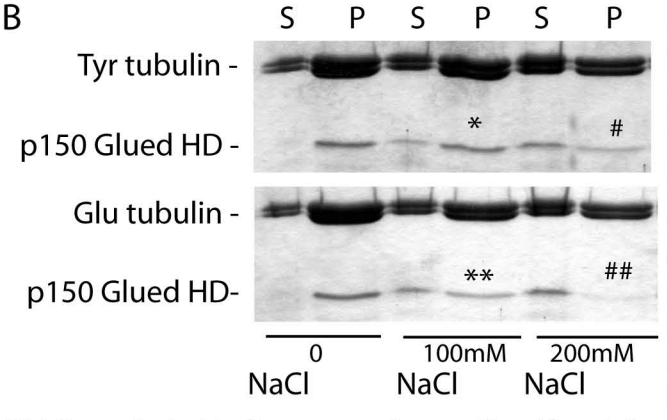

Figure 6: MT tip composition in WT and TTL KO fibroblasts. (A) Localization of CLIP-115, p150 Glued, MCAK and CLASP at EB1 labelled microtubule tips, in WT or TTL KO cells. Cells were transfected with GFP-CLIP-115, or GFP-p150 Glued, or GFP-MCAK and or GFP-CLASP cDNA, and double stained with GFP and EB1 antibodies. More than 50 cells were examined in each genotype for each condition. In WT fibroblasts, all expressed proteins showed a comet like distribution at MTs tips. In TTL KO fibroblasts, CLIP-115 and p150Glued did not decorate MT tips and showed a diffuse distribution in the cytoplasm. Scale bar: 10um.

(B) Microtubule-binding assay of p150 Glued head domain. p150 Glued head domain (p150 GluedHD) was co-polymerized with Tyr or Glu tubulin. Tyr and Glu-MTs were stabilized with Taxol and incubated with increasing concentrations of NaCl, as indicated. Equal amount of supernatants (S) and pellets (P) were separated by SDS/PAGE and stained with Coomassie blue. p150 GluedHD showed a band with a molecular mass of 25 kD. In the presence of 100 mM NaCl, the bulk of p150 GluedHD remained bound to Tyr-MTs (*) whereas only about half of p150 GluedHD remained bound to Glu-MTs (**). In the presence of 200 mM NaCl, a sizeable proportion of p150 GluedHD was still bound to Tyr-MTs (#) whereas only a very small proportion of p150 GluedHD remained bound to Glu-MTs (##).

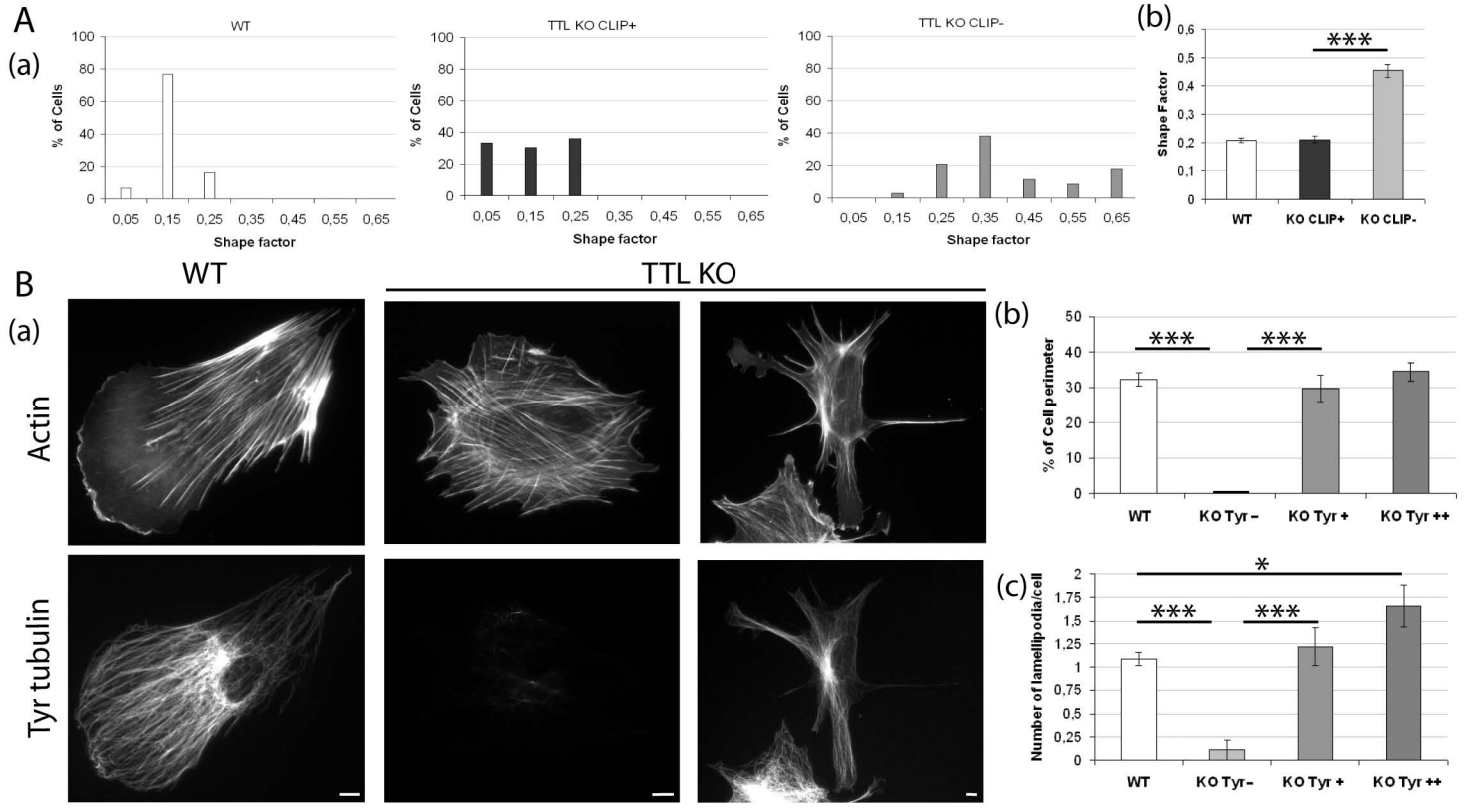

Figure 7: Morphological analysis of WT or TTL KO fibroblasts.

(A) Morphology: a shape factor (4π area/perimeter²) was determined in WT or TTL KO fibroblasts. (a) Shape factor distribution in WT (n=43), TTL KO CLIP+ (n=36) or TTL KO CLIP– fibroblasts (n=34). Note that TTL KO population showed a bimodal shape factor distribution. (b) Shape factor mean values + - S.E.M. Compared to WT or to CLIP+ TTL KO fibroblasts, CLIP- TTL KO cells exhibited a significant increase in the shape factor, *** $p < 0.001$ (t test).

(B) Polarization: (a) representative images of WT or TTL KO fibroblasts double stained for actin and Tyr tubulin. WT cell showed a polarized morphology with a large lamellipodia. In contrast, Tyr – TTL KO fibroblast showed no polarization and abundant stress fibers. Tyr+ TTL KO fibroblasts generally presented two or more lamellipodia. Scale bar: 10um. (b) Quantitative analysis of the percentage of cell perimeter occupied by lamellipodia in WT (n=68) or Tyr–, Tyr+, Tyr+ + TTL KO cells (n=83). *** $p<0.001$ (t test). (c) Number of lamellipodia per cell in WT (n=68) or Tyr–, Tyr+/-, Tyr+ + TTL KO cells (n=83). Tyr+ + TTL KO cells exhibited an increase of the number of large lamellipodia extensions compared to WT fibroblasts. * $p<0.05$*** $p<0.001$ (t test).

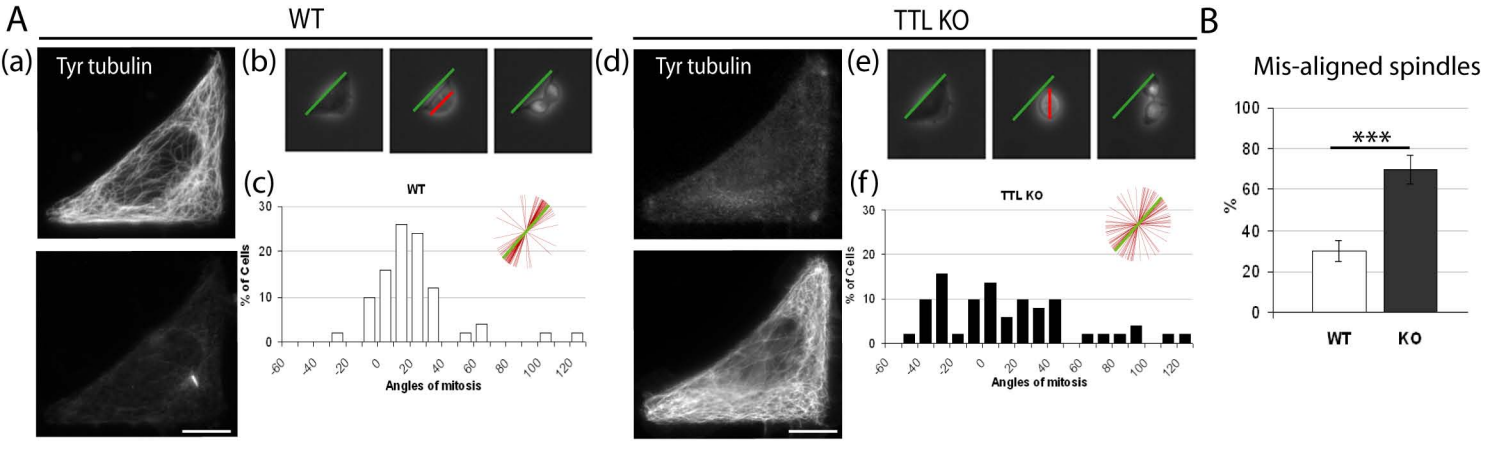

Figure 8: Mitotic spindle orientation in WT or TTL KO fibroblasts.

(A) Double-immunostaining of Tyr and Glu tubulin in a WT (a) or TTL KO (d) interphase fibroblasts grown on an L shaped fibronectin micropattern. Scale bar: 10um. (b,e) Example of time-lapse acquisition of a WT (b) or a TTL KO (e) cells during mitosis. Time-lapse pictures were used to measure the mitotic angle (red line) in function of the hypotenuse angle of the pattern (green line).(c, f) The distribution of mitotic angles in WT (c)(n=50) and TTL KO (f) (n=51) populations is shown. TTL KO cells showed a disperse spindle orientation compared to WT cells. (B) Percentages of mis-aligned spindles (spindle angle deviating by more than 15° from the median value in WT (n=50) or TTL KO populations (n=51). TTL KO fibroblasts exhibited a large increased of mis-aligned spindles compared to WT cells, ***$p<0.001$ (t test).

Supplementary Data

Figure S1: GFP-CLIP-170 over-expression in WT fibroblasts

WT fibroblasts were transfected with GFP-CLIP-170 cDNA and triple stained with Tyr tubulin, EB1 and GFP antibodies. Note that in WT cells expressing high levels of CLIP-170, the presence of large aggregates did not preclude CLIP-170 association with microtubule ends. Scale bar: 10 um.

Figure S2: Microtubule Growth rate in a WT fibroblast. Images of a WT cell expressing EB3-RFP and GFP-CLIP170 cDNAs were collected every 3 seconds in each channel.

Figure S3 Microtubule Growth rate in a TTL KO CLIP+ fibroblast. Images of a TTL KO cell expressing EB3-RFP and GFP-CLIP170 cDNAs were collected every 3 seconds in each channel. GFP-CLIP-170 showed a widespread distribution throughout the cell, with most EB3-RFP positive microtubule tips being also positive for GFP-CLIP-170.

Figure S4: Microtubule Growth rate in a TTL KO CLIP– fibroblast. A TTL KO cell was double transfected with EB3-RFP and GFP-CLIP170 cDNAs. CLIP-170 mis-localization was evident by the presence of GFP-CLIP-170 aggregates that didn’t interfere in MT growth rate measured with EB3-RFP positive MT tips. Images were collected every 3 seconds in each channel.